 DOI: 10.17344/acsi.2017.3613 *Acta Chim. Slov.* **2018,** *65,* 86–96

Scientific paper

Spectroscopic, Structural and Density Functional Theory (DFT) Studies of Two Oxazol-5-one Derivatives

İbrahim Hanif Nazlı,[1] Duygu Barut Celepci,[2,*] Gül Yakalı,[3] Derya Topkaya,[4] Muhittin Aygün[2] and Serap Alp[4]

[1] *Dokuz Eylül University, Graduate School of Natural and Applied Science, Izmir, TURKEY*

[2] *Dokuz Eylül University, Faculty of Science, Department of Physics, Izmir, TURKEY*

[3] *Akdeniz University, Serik Gülsün-Süleyman Süral Vocational School of Higher Education, Department of Opticianry Program, Antalya, TURKEY*

[4] *Dokuz Eylül University, Faculty of Science, Department of Chemistry, Izmir, TURKEY*

** Corresponding author: E-mail: duygu.barut@deu.edu.tr*

Received: 06-06-2017

Abstract

In this study, two oxazol-5-one derivatives, $C_{20}H_{20}N_2O_2$ (**1**) and $C_{21}H_{22}N_2O_2$ (**2**), were synthesized by getting condensed *p-N,N*-diethylaminobenzaldehyde with two presented hippuric acid derivatives and in further studies they were analysed spectrochemically. Molecular and crystal structures of the compounds were determined by single-crystal X-ray diffraction and the results revealed that the molecular packing of the crystal structures were stabilized by weak intra- and intermolecular interactions also with C–O···π, C–H···π and π···π stacking interactions. Computational studies were also performed using DFT method at B3LYP/6-311G(d,p) level of theory. Vibrational modes and chemical shifts were calculated and compared with the experimental data. In addition, frontier molecular orbitals and molecular electrostatic potential surfaces were simulated. The calculated results show that the optimized geometries can well reproduce the crystal structure. Purpose of this study was to survey the effects of the reactants, which were condensed with each other to produce oxazol-5-one, upon the characteristic properties and crystal forms of the final oxazol-5-one.

Keywords: Oxazol-5-one, Crystal structure, DFT, Frontier molecular orbitals

1. Introduction

Variety of amino acids and of course peptides can be synthetically obtained from glycine with the classical Erlenmeyer–Plöchl azlactone synthesis.[1–5] Due to the five -membered heterocyclic core, oxazol-5-ones are biologically active molecules and widely used in biomedicinal applications.[6–9] Oxazol-5-ones have found important roles as drugs, enzyme inhibitors and fluorescent sensors.[7–10] Oxazol-5-ones are also used in dye industry owing to the fact that oxazol-5-ones are easily obtainable in crystalline states and they possess promising photochemical/photophysical properties due to their chromophore group.[10,11] Herein, we report on the synthesis, spectral characterization and theoretical studies of two oxazol-5-one derivatives. The experimental FT-IR, ^{1}H NMR, ^{13}C NMR studies were performed. Structures of the compounds were confirmed by single-crystal X-ray diffraction studies. Theoretical calculations were also carried out in order to corroborate the experimental results.

1. 1. Synthesis of Oxazol-5-one

Generally oxazol-5-ones are synthesized by Erlenmeyer–Plöchl azlactone reaction. Hippuric acid (*N*-benzoylglycine) derivatives turn into 2-aryloxazol-5-ones in the presence of acetic anhydride as the reaction media, besides the addition of sodium acetate, acetic anhydride and aromatic aldehydes they condense into 2-aryl-4-arylmethyleneoxazol-5-ones which are known as unsaturated azlactones.

2. Materials and Methods

Some reagents (toluene, ethanol, ethyl acetate, sodium acetate, *p-N,N*-diethylaminobenzaldehyde) were obtained

from commercial sources and used without further purification, acetic anhydride was purified by distillation, hippuric acid derivatives were synthesised and used after purification.

2. 1. Analytical Instruments and Spectroscopy Techniques

Melting points were determined by Barnstead Electrothermal 9,100 instrument. FT-IR spectra were recorded by Perkin–Elmer Spectrum BX FTIR spectrometer using KBr pellets. NMR data were measured by Varian 3.2 400 MHz spectrometer in $CDCl_3$ solutions and chemical shifts were expressed in ppm downfield from tetramethylsilane.

2. 2. Synthesis

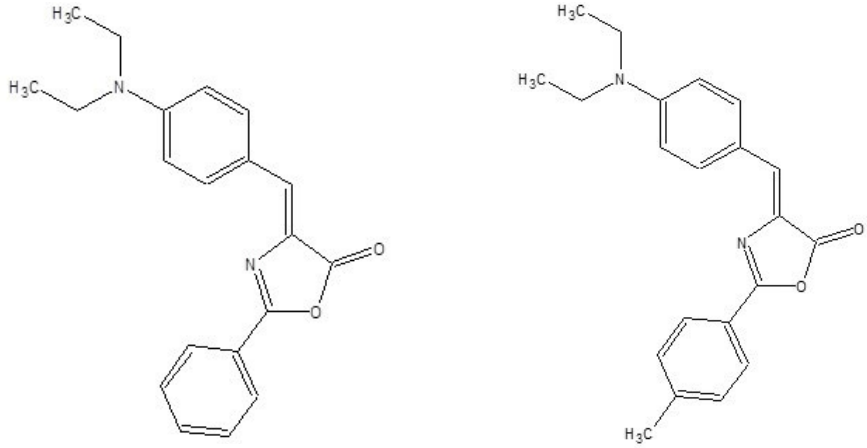

Scheme 1. Chemical diagrams of the compounds **1** and **2**.

2. 2. 1. Synthesis of 4-(*p*-*N*,*N*-Diethylaminophenylmethylene) -2-phenyloxazol-5-one (1)

2.82 mmol *p*-*N*,*N*-diethylaminobenzaldehyde, 2.82 mmol *N*-benzoylglycine (hippuric acid) and 2.82 mmol sodium acetate was added to 3 mL of redistilled acetic anhydride. Reaction mixture was stirred under dry conditions for 4–5 hours at 100 °C, thereafter stirred at room temperature overnight. 3 mL of ethanol was added to cooled oily-solid like mixture and left in refrigerator for 2–3 hours. Precipitation occurred so that mixture was filtered, solid obtained washed with ethanol and recrystallized from hexane–ethyl acetate solution. Determined melting point of **1** is 134.5 °C.

2. 2. 2. Synthesis of 4-(*p*-*N*,*N*-Diethylaminophenylmethylene)-2-(*p*-tolyl)oxazol-5-one (2)

p-*N*,*N*-Diethylaminobenzaldehyde (5.18 mmol), *p*-toluoylglycine (5.18 mmol) and sodium acetate (5.18 mmol) was added to 4 mL of redistilled acetic anhydride. Reaction mixture was stirred under desiccant for 4–5 hours at 100 °C and stirred at room temperature overnight. 3 mL of ethanol was added to cooled oily-solid like mixture and was put into fridge for 2–3 hours. Precipitate was filtered, washed with ethanol, and recrystallized from toluene. Determined melting point of **2** is 153.9 °C.

2. 3. X-Ray Crystallography

Single crystal X-ray diffraction data of (4*Z*)-4-(*p*-*N*,*N*-diethylaminophenylmethylene)-2-phenyloxazol-5-one (**1**) and (4*Z*)-4-(*p*-*N*,*N*-diethylaminophenylmethylene)-2-(*p*-tolyl)oxazol-5-one (**2**) were collected at room temperature on an Rigaku-Oxford Xcalibur diffractometer with an Eos-CCD detector using graphite-monochromated Mo-Kα radiation (λ = 0.71073 Å). Data collections and reductions along with absorption corrections were performed using CrysAlis*Pro* software package.[12] Structure solutions were performed using SHELXT embedded in the Olex2.[13,14] Refinement of coordinates and anisotropic thermal parameters of non-hydrogen atoms were carried out by the full-matrix least-squares method in SHELXL.[15] All hydrogen atoms of both compounds were placed in geometrically idealized positions (C–H = 0.93–0.96–0.97 Å). The details of the crystal data, data collection and structure refinement of the compounds are summarized in Table 1.

2. 4. Computational Details

The synthesized compounds **1** and **2** have been optimized at DFT/B3LYP method, using 6-311G(d,p) basis set. Also, the harmonic vibrational frequencies and NMR spectra were calculated at the same levels of theory for the optimized structures. The calculated frequencies were scaled down by using single scaling factor 0.9669 for DFT/B3LYP/6-311G(d,p) level, in order to improve the agreement with the experimental values.[16] The ^{1}H and ^{13}C iso-

Table 1. Crystal data and structure refinement parameters for the compounds **1** and **2**.

	1	**2**
Empirical formula	$C_{20}H_{20}N_2O_2$	$C_{21}H_{22}N_2O_2$
Formula weight	320.38	334.41
Temperature (K)	294 (2)	294 (2)
Crystal system / space group	Triclinic / *P-1*	Triclinic / *P-1*
Unit cell dimensions		
a (Å)	7.5779(7)	7.8711(6)
b (Å)	10.6860(11)	11.0322(9)
c (Å)	11.1813(9)	11.1509(8)
α (°)	108.647(9)	108.341(7)
β (°)	96.641(7)	99.513(6)
γ (°)	93.094(8)	90.893(7)
Volume (Å^3)	848.16(14)	904.10(13)
Z / D_{calc} (mg m^{-3})	2 / 1.254	2 / 1.228
Absorption coefficient (mm^{-1})	0.082	0.080
F (000)	340	356
Reflections collected / unique	4592 / 3197[R_{int} = 0.0187]	4692 / 3420[R_{int} = 0.0196]
Data / restrains / parameters	3197 / 0 / 219	3420 / 0 / 229
Goodness of fit on F^2	1.022	1.028
Final R indices [$I > 2\sigma(I)$]	R_1 = 0.0495, wR_2 = 0.1030	R_1 = 0.0486, wR_2 = 0.1092
R indices (all data)	R_1 = 0.0782, wR_2 = 0.1193	R_1 = 0.0733, wR_2 = 0.1238
Largest difference peak and hole (eÅ^{-3})	0.145 / –0.172	0.164 / –0.179

tropic shielding tensors referenced to the TMS calculations were performed by using gauge invariant atomic orbital (GIAO) method in chloroform solvent.[17] Highest occupied molecular orbital (HOMO), lowest unoccupied molecular orbital (LUMO) and MEP have been calculated from optimized geometry of the molecules. All calculations were carried out with the Gaussian 09W and Gauss View molecular visualization program.[18,19]

3. Results and Discussions

3. 1. Crystal Structure

The atomic numbering scheme of the crystal structures and the optimized geometries which has the most favourable conformation of the compound **1** and **2** are shown in Figures 1a and b. Molecules crystallize in triclinic system with *P-1* space group. Selected bond distances, bond angles and torsion angles together with corresponding values obtained by means of X-ray crystallographic analysis and DFT calculations are compared and listed in Table 2.

The structures of the title compounds comprise of a *p-N,N*-diethylaminophenylmethylene fragment bridged by the methine C4 atom and an oxazol-5-one ring, linked to the phenyl ring in compound **1**, whereas the *p*-tolyl moiety in **2**. The oxazol-5-one rings are almost planar for both compounds, with a r.m.s. deviation of –0.006(2) Å for **1** and 0.004(1) Å for **2**. Phenyl rings are twisted slightly out of these planes, with the dihedral angles between two rings being 12.80(2)^0 and 6.41(2)^0, respectively. Similarly, there is a twist between the *p-N,N*-diethylaminophenyl moiety and oxazol-5-one ring [dihedral angles are 18.89(2)^0 and 17.71(2)^0; C4/C5/C10/C9 torsion angles are –175.68(1)^0 and 173.58(1)^0, respectively], that are linked through the C3=C4 double bonds. The olefinic C3=C4 double bond lengths [1.347(1) Å for **1** and 1.354(1) Å for **2**] are slightly longer than the formal C=C bond, but mostly consistent with double bonds in similar studies.[20–23] The molecules adopt a *Z* conformation about these olefinic bonds with C5 *cis* to N1. C2=O2 bond distances are also shown to have a typical double bond character with lengths of 1.196(1) Å and 1.201(1) Å, respectively.[24] The C3-C4-C5 angles are 129.90(1)^0 and 129.62(1)^0, respectively, being quite large. These angle values and the exocyclic angles of C3 and C5 (Table 2) are in accordance with the repulsive intramolecular interactions between the N1 and H10 atoms, similar to the oxazol-5-one derivatives reported previously.[25–27] Bond lengths, angles and torsion angles of **1** and **2** are comparable with the similar compounds, especially for the oxazol-5-one rings, O1-C2-O2 exocyclic bond angles and N1/C3/C4/C5 torsion angles. Except the torsion angles, the bond parameters are comparable with the other oxazol-5-one derivatives.[28–32] N1/C3/C4/C5 torsion angles [–7.78(1) Å for **1** and 8.39(1) Å for **2**] are slightly different. Also, as can be seen from the results, there is a good correlation between the experimental and theoretical data. The observed differences can be attributed to the fact that while the theoretical calculations are made for an isolated molecule in the gas phase, the experimental results obtained are those of the molecules in the solid state.

In the compound **1,** there are only weak C-H···O intermolecular interactions and C-H···N intramolecular interactions. In addition, there are strong C-O···π interacti-

ons [Cg3: C15-C20; O···Cg3: 3.786(4) Å; symmetry code (ii): –*x*, 2–*y*, 1–*z*], two strong π···π interactions with 3.34(2) Å distance between the centroids Cg1···Cg1 and 3.85(2) Å distance between the centroids Cg1···Cg3 [Cg1:O1/C1/N1/C3/C2; Cg1···Cg1 symmetry code (iii): 1–*x*, 2–*y*, 1–*z*; Cg1···Cg3 symmetry code (iv): –*x*, 2–*y*, 1–*z*]. The compound **1** consists of a dimeric arrangement of molecules around an inversion centre formed via a C-H···O intermolecular hydrogen bond linking the molecules along the *a* axis (Figure 2). This centrosymmetric hydrogen-bonded dimers are formed with an (22) ring motif.[33]

Molecular packing in the crystal structure of the compound **2** was determined by the weak intramolecular C–H···N and C–H···O interactions, C–H···π stacking interactions and van der Waals forces. Molecules are linked to each other through the C–H···π interaction between the methyl H21C atom and *p*-*N*,*N*-diethylaminophenyl moiety of the adjacent molecule with C21-H21C···Cg2^{v}

Table 2. Selected interatomic distances (Å), angles and torsion angles (°) for the compounds **1** and **2** as observed experimentally and as calculated using DFT/ B3LYP/6-311G(d,p) method.

Compound	**1**		**2**	
Bond Lengths	**Experimental**	**Calculated**	**Experimental**	**Calculated**
C1–O1	1.374(1)	1.372	1.382(1)	1.374
C2–O1	1.394(1)	1.413	1.396(1)	1.412
C2–O2	1.196(1)	1.197	1.201(1)	1.197
C1–N1	1.280(1)	1.291	1.287(1)	1.292
C3–N1	1.398(1)	1.396	1.400(1)	1.396
N2–C8	1.357(1)	1.376	1.364(1)	1.377
N2–C11	1.452(1)	1.463	1.459(1)	1.462
N2–C13	1.453(1)	1.462	1.456(1)	1.462
C3–C4	1.347(1)	1.362	1.354(1)	1.361
C4–C5	1.430(1)	1.436	1.437(1)	1.437
Bond Angles				
C1–N1–C3	105.55(1)	105.80	105.63(1)	105.811
N1–C3–C2	108.31(1)	108.66	108.31(1)	108.658
N1–C3–C4	128.16(1)	129.20	128.50(1)	129.238
N1–C1–O1	115.85(1)	115.79	115.73(1)	115.757
N1–C1–C15	127.22(1)	127.14	127.26(1)	127.192
C1–O1–C2	105.46(1)	105.92	105.44(1)	105.940
O1–C2–O2	121.31(1)	122.10	121.44(1)	122.107
O1–C2–C3	104.80(1)	103.80	104.87(1)	103.834
O2–C2–C3	133.88(1)	134.1	133.67(1)	134.059
O1–C1–C15	116.88(2)	117.07	117.00(1)	117.051
C8–N2–C11	121.38(1)	121.87	121.44(1)	121.853
C8–N2–C13	122.41(1)	121.95	121.71(1)	121.971
C11–N2–C13	116.15(1)	116.17	116.78(1)	116.174
N2–C8–C7	121.74(1)	121.66	121.67(1)	121.667
N2–C8–C9	122.00(1)	121.62	121.93(1)	121.634
N2–C11–C12	113.15(1)	113.97	113.39(1)	113.942
N2–C13–C14	112.40(1)	121.87	112.55(1)	113.968
C3–C4–C5	129.90(1)	130.33	129.62(1)	130.302
C4–C5–C10	123.78(1)	124.22	124.01(1)	124.257
Torsion Angles				
O1–C1–C15–C16	–11.87(1)	–0.56(2)	6.57(1)	0.460
N1–C1–C15–C16	170.39(1)	179.46	–174.42(1)	–179.530
N1–C1–C15–C20	–10.81(1)	–0.55	5.57(1)	0.566
N1–C3–C4–C5	–7.78(1)	–0.18	8.39(1)	0.167
C3–C4–C5–C6	170.69(1)	179.70	–174.73(1)	–179.798
C4–C5–C10–C9	–175.68 (1)	–179.90	173.58(1)	179.919
O2–C2–C3–C4	–0.94(1)	0.015	0.83(1)	–0.053
C7–C8–N2–C11	7.01(1)	–5.70	–6.36(1)	5.335
C9–C8–N2–C13	4.42(1)	–5.64	–3.62(1)	5.812

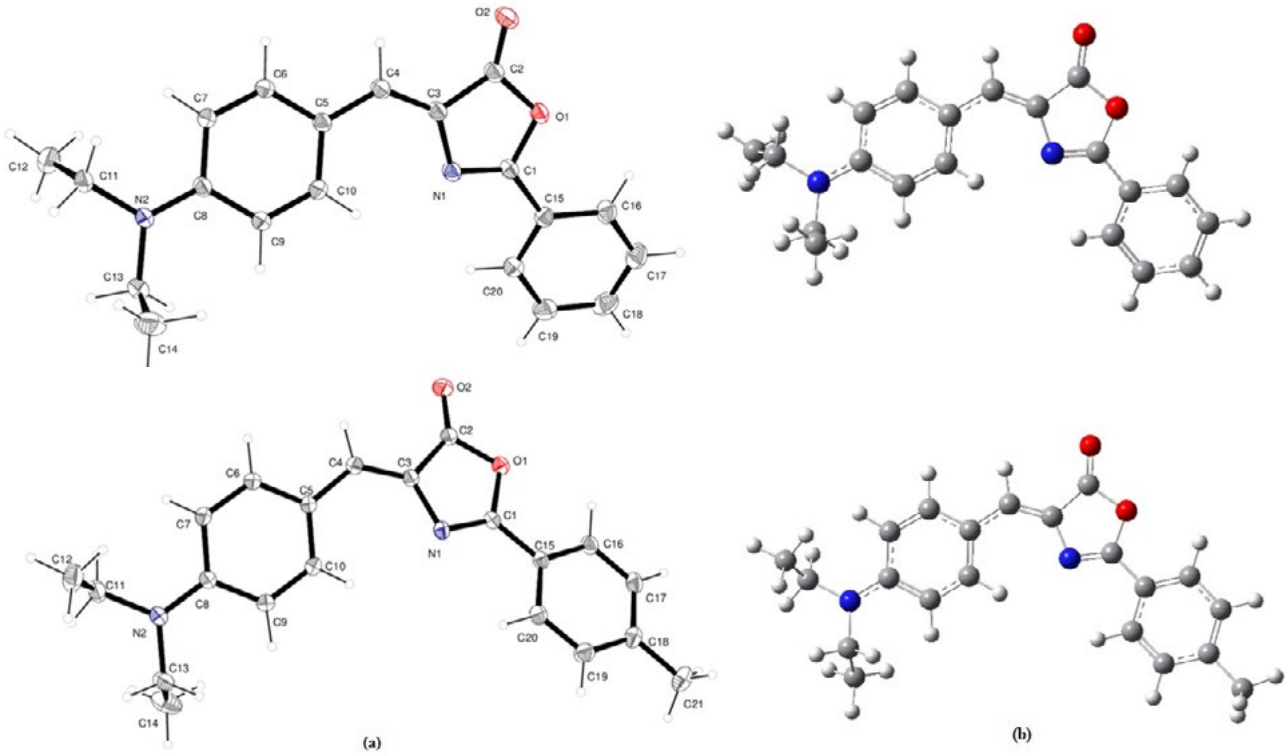

Figure 1. (a) The molecular structure of the compounds **1** and **2** with atom numbering scheme and 30% probability displacement ellipsoids and **(b)** optimized structures for DFT/ B3LYP/6-311G(d,p) level.

Table 3. Hydrogen bonds (Å, °).

Molecule	D–H···A	D–H	H···A	D···A	D–H···A
1	C10–H10···N1	0.93	2.46	3.088(3)	125
	C16–H16···O1	0.93	2.49	2.8001(3)	100
	C11–H11A···O2^{i}	0.97	2.56	3.4428(4)	151
2	C10–H10···N1	0.93	2.45	3.0930(3)	126
	C16–H16···O1	0.93	2.48	2.8030(2)	101
	C21–H21C···Cg2^{v}	0.96	2.97	3.8267(3)	149

Symmetry codes: (i) 1–*x*,1–*y*,1–*z*; (v) *x*, *y*, 1+*z*.

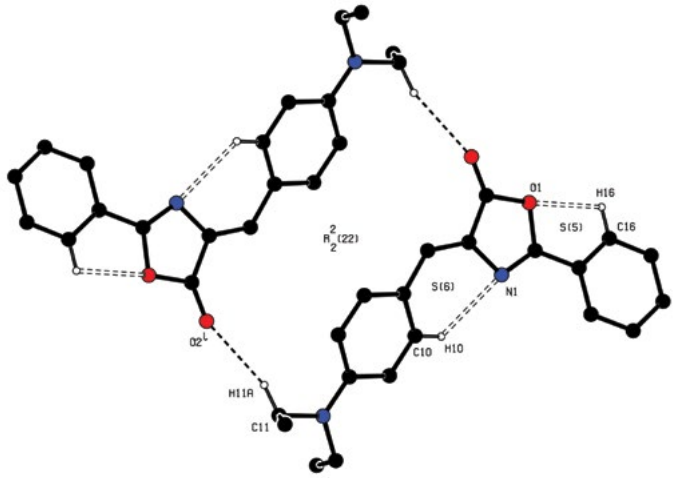

Figure 2. The formation of the hydrogen bond motif through C11–H11A···O2^{i} hydrogen bonds for the compound **1** [^{i} 1+*x*, 1+*y*, +*z*]. For the sake of clarity, H atoms not involved in the motif have been omitted, and only the interacting atoms are labeled.

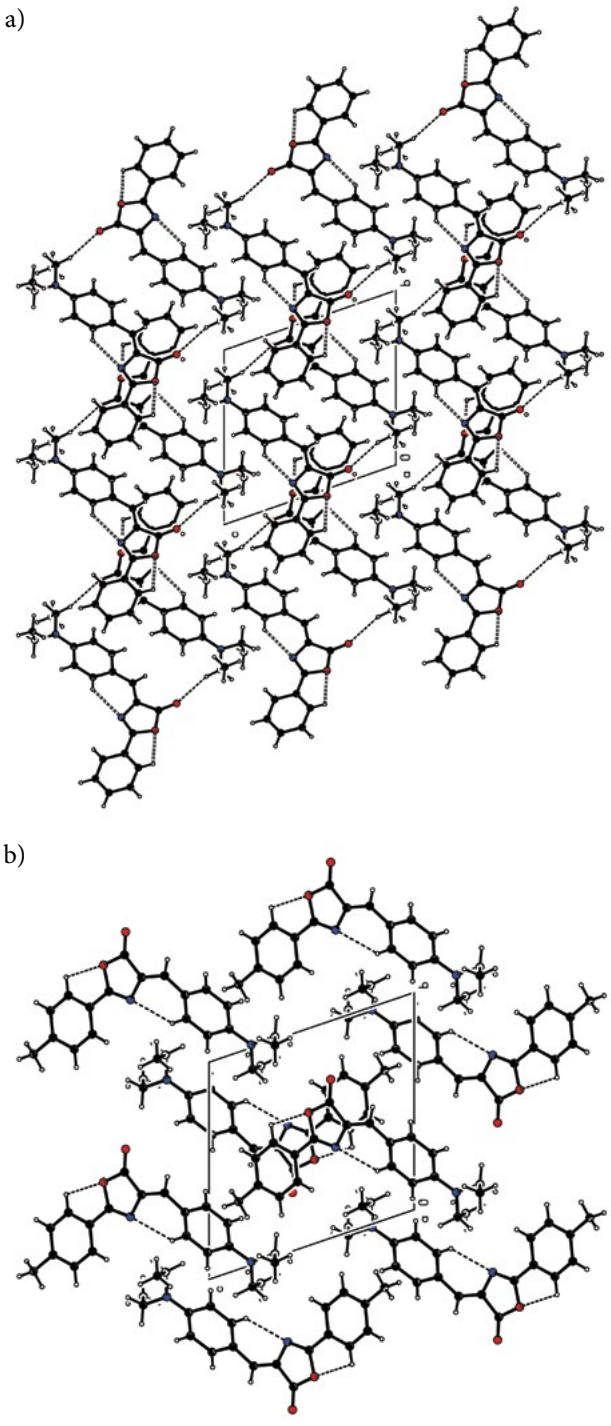

Figure 3. (a) A view along the *a* axis of unit cell showing the intermolecular hydrogen bonding interactions and formation of (22) ring motif belongs to the compound **1**. **(b)** A view along the *a* axis of the crystal packing of the compound **2**.

separation of 2.97 Å [Cg(2): C5-C10]. For both compounds, intermolecular and intramolecular interactions and C–H···π interactions with their symmetry codes are listed in Table 3 and crystal packing diagrams are given in Figures 3a and b.

3. 2. Frontier Molecular Orbitals

The highest occupied molecular orbital (HOMO) and lowest unoccupied molecular orbital (LUMO) are the basic orbitals that play an important role in chemical stability. The HOMO shows the ability to donate an electron, whereas the LUMO as an electron acceptor shows the ability to obtain an electron. This also predicts the nature of electrophiles and nucleophiles at the atom where the HOMO and LUMO are stronger.[34] The energy gaps of the compounds **1** and **2** were calculated using B3LYP/6-311G(d,p) level (Figure 4). For both compounds, highest electron density lies mainly on the oxazol-5-one ring and on (diethylamino)benzylidene moiety. The HOMO energy levels are calculated at –5.271(2) and –5.214 eV, respectively. On the other hand, the electrons are more distributed over the phenyl for the LUMO with the energy of –2.27 and –2.203 eV, respectively. The energy gaps of HOMO and LUMO could be determined to be about 3.001 eV for the compound **1** and 3.011 eV for **2**, which indicate the molecules become less stable and more reactive.

3. 3. Molecular Electrostatic Potential

The molecular electrostatic potential (MEP) is a reactivity map displaying probable region for the electrophilic and nucleophilic attacks and hydrogen bonding interactions of the molecules.[35] In order to predict the reactive part of the electrophilic and nucleophilic attack, the MEP of the title compounds were also calculated from B3LYP/6-311G(d,p) optimized geometry. In the compounds **1** and **2**, the negative regions (red) of the MEP which are around the O2 and O1 atoms bounded to oxazol-5-one ring, were related to electrophilic reactivity that is responsible for intermolecular hydrogen bonding for compound **1**, intramolecular hydrogen bonds for compound **2** and positive regions (blue) which are around the hydrogen atoms correspond to nucleophilic reactivity (Figure 5).

3. 4. Analysis of the Vibrational Spectra

The infrared spectra of the title compounds were recorded in the 4000–600 cm^{-1} region using FT-IR spectrophotometer and are presented in Figure 6. The vibrational band assignments were determined at B3LYP/6-311G(d,p) theory level. It is well-known that the vibrational wavenumbers obtained by DFT computations usually overestimate their experimental counterparts. These discrepancies can be corrected either by computing anharmonic corrections or by introducing a scaled field.[36] The visual check for the vibrational band assignments were also performed by using GaussView molecular visualization program. There are no negative frequencies in the calculated IR spectra, which indicates a stable optimized geometry. The selected harmonic vibrational IR frequencies and the corresponding experimental values are listed in Table 4. The infrared spectra of the compounds have some

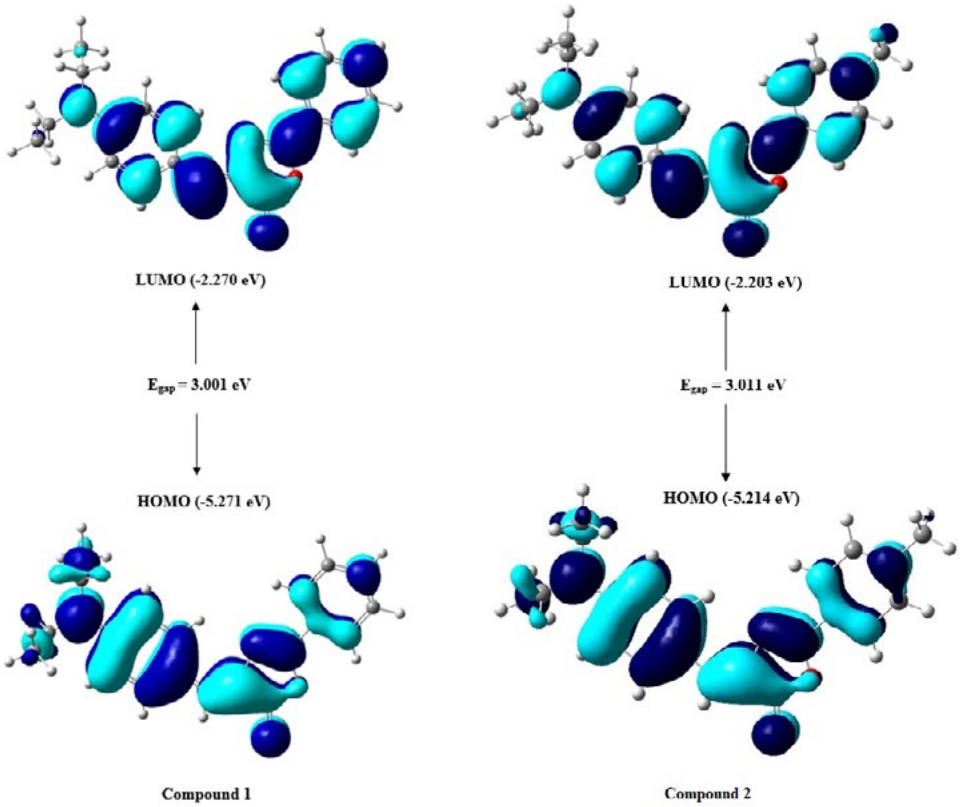

Figure 4. Frontier molecular orbital surfaces and energy levels for the HOMO and LUMO of the compounds **1** and **2** computed at B3LYP/6-311G(d,p) level.

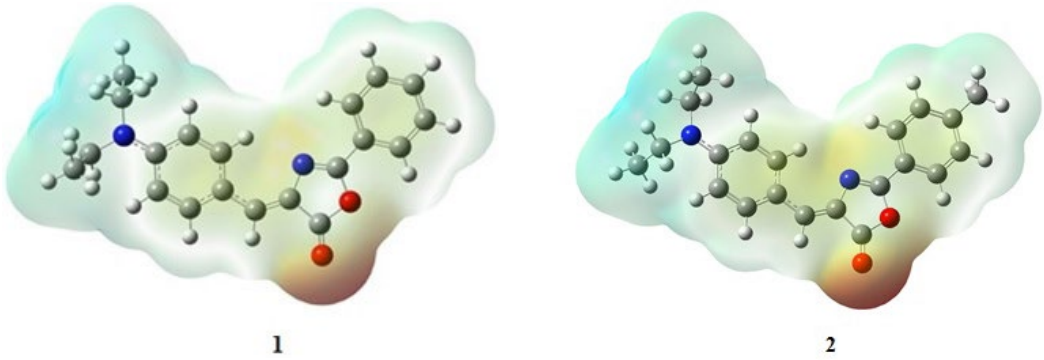

Figure 5. Molecular electrostatic potential surface (MEP) of the compounds **1** and **2**.

characteristic bands of the stretching vibrations of the =C–H, –C–H, C=O, C=C–O etc. groups, in plane bending vibrations of C–H, C–H_2, C–H_3 groups and out of plane bending vibrations for =C–H, C–H_3 groups. In addition to these vibrations, some wagging, scissoring, twisting and rocking vibrations are obtained by theoretical study. There are some discrepancies between the observed and calculated data. This is because the experimental data were taken as KBr pellets, whereas the theoretical calculations were performed for isolated molecule in the gaseous phase.

The most characteristic bands of aliphatic –CH_2– and –CH_3 groups are those arising from C–H stretching vibrations which experimentally occur in general region of 3000–2840 cm^{-1}. The asymmetrical/symmetrical stretching for –CH_2– groups is observed near 2926/2853 cm^{-1} and for –CH_3 groups near 2962/2872 cm^{-1}, respectively. These standard values can be slightly changed depending on the surrounding of the alkyl moiety. Besides the aromatic C–H stretching bands which occurred at 3100–3000 cm^{-1}, all obtained experimental C–H bending vibrational data are compatible with expected values as well as stretching vibrational data.

C–H stretching vibrations were calculated at 3106/3104 cm^{-1} for symmetric and 3081/3063 cm^{-1} for

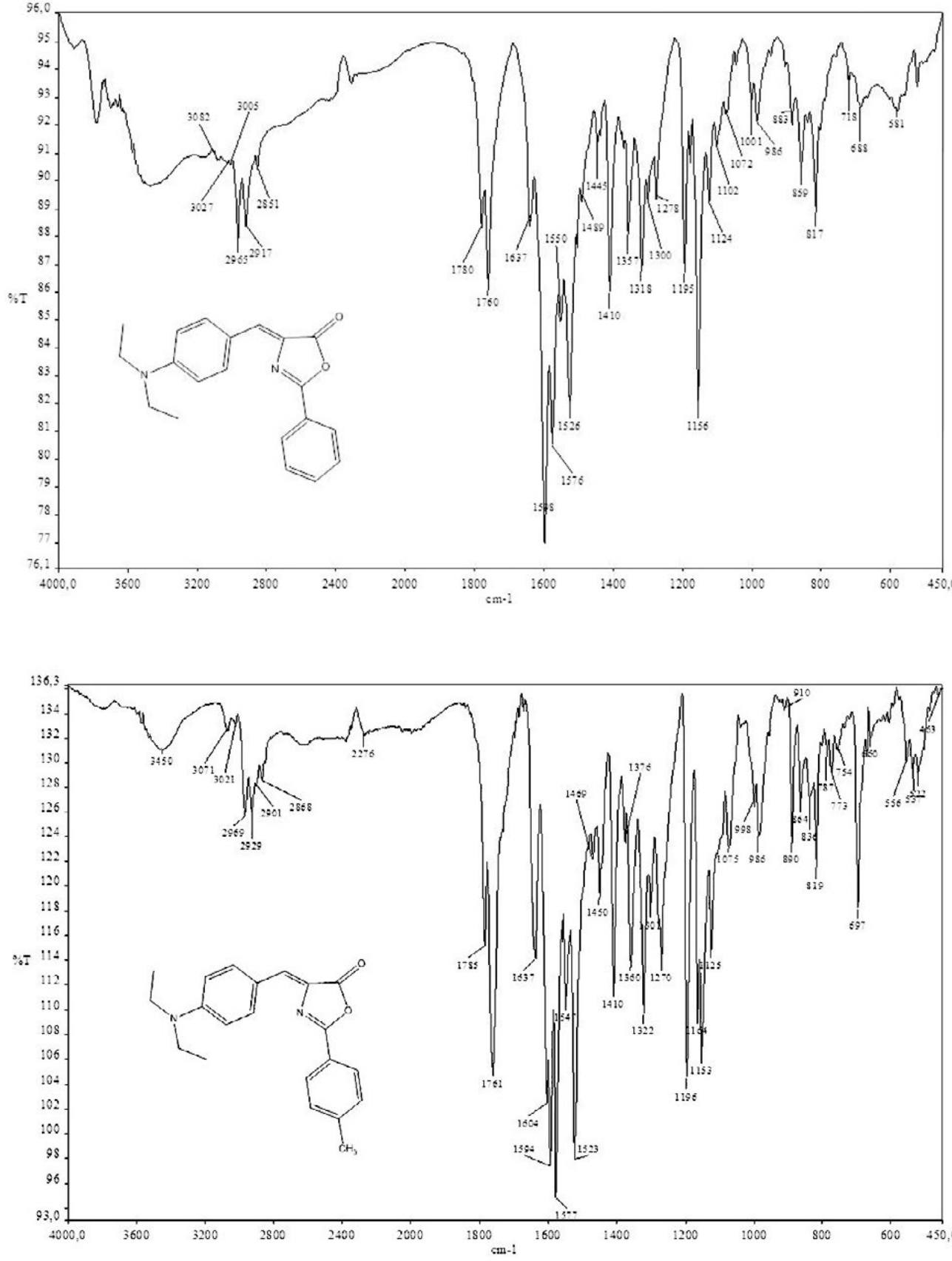

Figure 6. IR spectra of the title compounds **1** (above) and **2** (below).

Table 4. Comparison of the observed and calculated vibrational spectrum of the compounds.

Bond assignment[a]	IR, cm^{-1} (experimental)		Scaled frequency, cm^{-1} (calculated B3LYP/6-311G(d,p)	
	1	**2**	**1**	**2**
ν_{sym}(C-H)$_{aromatic}$	3021	3027	3106	3104
ν_{asym}(C-H$_2$)	2929	2917	3092	3102
ν_{asym}(C-H$_3$)	2969	2965	3100	3099
ν_{asym}(C-H)$_{aromatic}$	3071	3082	3081	3063
ν(C-H)	–	–	3047	3046
ν_{sym}(C-H$_2$)	2886	2851	3043	3043
ν_{sym}(C-H$_3$))	2901	2901	3038	3028
ν(C=O)	1785	1780	1857	1795
ν(C=C)	1637	1637	1646	1632
α(C-H)$_{aromatic}$	1594	1598	1599	1592
α(C-H$_2$)	1469	1489	1457	1496
γ(C-H)$_{aromatic}$	–	–	1459	1457
Γ(C-H$_3$)	1450	1445	1449	1451
β(C-H$_3$)	1360	1357	1352	1351
ω(C-H$_2$)	1322	1318	1349	1349
τ(C-H$_2$)	1270	1278	1275	1278
ν(C-C-H$_3$)	1196	1195	1179	1191
γ(C-H)	1124	1125	1131	1133
τ(C-H)$_{aromatic}$	890	883	930	928
Γ(C-H)	–	–	925	926
ω(C-H)$_{aromatic}$	819	817	800	811
γ(C-H$_2$)	754	718	769	766

[a] Abbreviations: ν-stretching; β-in plane bending; α-scissoring; γ-rocking; Γ-out of plane bending; τ-twisting, ω-wagging. Subscripts: *asym*, asymmetric; *sym*, symmetric.

asymmetric bands which are in the characteristic region for the identification of C–H stretching vibrations in the compounds **1** and **2**, respectively. The symmetric stretching vibrations of C–H$_2$ are determined at 2886/2851 cm^{-1} and asymmetric stretching vibrations are determined at 2929/2917 cm^{-1}. Similarly, C–H$_3$ symmetric vibrational modes are observed at 2901 cm^{-1} for both compounds, whereas the asymmetric modes are identified at 2969/2965 cm^{-1}.[37] These results are considerably compatible with the experimental data.

Other characteristic bands C=O, C=C, etc. were also detected. As usually, carbonyl stretching band at five -membered heterocyclic core shows around 1780 cm^{-1}, C=C stretching bands at *exo* positions shows around 1640 cm^{-1}, experimentally. These two values are also overlapping with our experimental results. In contrast to experimental value, calculated ν(C=O) vibration band was detected quite high for compound **1** (1857 cm^{-1}). This can be attributed to the strong intermolecular hydrogen bond (C11–H11B···O2).

3. 5. ^{1}H and ^{13}C NMR Analysis

Experimental ^{1}H and ^{13}C NMR of the title compounds were recorded in $CDCl_3$. Theoretical calculations carried out in the chloroform solvent (with respect to TMS) at the B3LYP/6-311G(d,p) method by adopting GIAO method and compared to the experimental chemical shift values,

Table 5. Comparison of the experimental and calculated ^{1}H NMR values in chloroform.

Atom	Experimental		Theoretical (B3LYP/6-311G(d,p)	
	1	**2**	**1**	**2**
H4	7.19	7.17	4.66	6.56
H6	8.14	8.03	5.22	6.96
H7	6.72	6.72	3.44	6.17
H9	6.72	6.72	4.41	6.33
H10	8.14	8.03	6.24	8.81
H11A	3.45	3.45	0.71	2.99
H11B	3.45	3.45	0.48	2.66
H12A	1.23	1.23	2.62	0.64
H12B	1.23	1.23	3.04	0.35
H12C	1.23	1.23	4.25	0.82
H13A	3.45	3.45	0.69	3.03
H13B	3.45	3.45	0.51	2.67
H14A	1.23	1.23	4.22	0.85
H14B	1.23	1.23	1.00	0.39
H14C	1.23	1.23	2.71	0.66
H16	8.13	8.03	5.91	7.49
H17	7.50	7.29	5.26	6.91
H18	7.50	–	5.13	–
H19	7.50	7.29	5.73	7.04
H20	8.13	8.11	5.84	7.96
H21A	–	2.44	–	1.56
H21B	–	2.44	–	1.99
H21C	–	2.44	–	2.08

Table 6. Comparison of the experimental and calculated ^{13}C NMR values in chloroform.

Atom	Experimental		Theoretical (B3LYP/6-311G(d,p)	
	1	**2**	**1**	**2**
C1	160.20	160.44	160.79	161.74
C2	168.68	168.78	165.90	167.68
C3	132.15	132.79	125.28	127.82
C4	135.21	135.05	127.41	133.55
C5	121.07	121.14	119.11	123.47
C6	128.74	129.51	129.30	138.67
C7	111.36	111.34	101.28	110.11
C8	150.11	149.97	150.99	152.29
C9	111.36	111.34	104.00	111.48
C10	128.74	129.51	128.17	136.11
C11	44.68	44.66	28.08	42.93
C12	12.64	12.64	14.29	7.69
C13	44.68	44.66	30.76	42.99
C14	12.64	12.64	9.85	7.97
C15	126.40	123.61	125.70	125.27
C16	127.74	127.95	121.54	129.34
C17	127.67	127.70	120.31	130.12
C18	133.44	142.92	121.42	146.57
C19	127.67	127.70	121.90	130.30
C20	127.74	127.95	122.30	128.43
C21	–	21.79	–	19.20

are presented in Tables 5 and 6. For the B3LYP/6-311G(d,p) method, the chemical shift value of tetramethylsilane (TMS) $\sigma_0(^{13}C)$ = 179.7024 ppm and $\sigma_0(^{1}H)$ = 31.3919 ppm was obtained.[38] For the compound **1**, NMR spectral data show that the C2 atom has the highest chemical shift value (168.68 ppm), whereas the methyl C12 and C14 atoms have the least one (12.64 ppm). Similarly in **2**, the highest chemical shift is for C2 with the value of 168.78 ppm and the least for C12 and C14 atoms at the range of 12.64 ppm. In the experimental spectrum, the signal of the C18 atom of the phenyl moiety was observed at 133.44 ppm in the compound **1**. But this value is higher in the **2** (142.92 ppm), because of the presence of a methyl group. ^{1}H NMR chemical shift values are calculated at 0.48–6.24 and 0.35–7.96 ppm for **1** and **2**, respectively. They are experimentally observed at 1.23–8.14 and 1.23–8.11 ppm, respectively.

4. Conclusions

Compounds **1** and **2** have been synthesized and characterized by FT-IR, ^{1}H NMR, ^{13}C NMR and X-ray single -crystal diffraction. In addition, density functional modelling studies of the oxazol-5-one derivatives have been reported in this study. The calculated geometric parameters by using the DFT with the 6-311G(d,p) basis set are mostly compatible with the X-ray structure. The vibrational band assignments and NMR shift values were performed at the same theory level to compare the experimental and calculated values of the compounds. These calculated and experimental results are in good agreement with the explanatory differences.

5. Acknowledgment

The authors acknowledge Dokuz Eylül University for the use of the Oxford Rigaku Xcalibur Eos Diffractometer (purchased under University Research Grant No: 2010. KB.FEN.13).

6. Supplementary Material

Crystallographic data as .cif files for the structures reported in this paper have been deposited at the Cambridge Crystallographic Data Center with CCDC 1547713 for compound **1** and 1547714 for **2**. Copies of the data can be obtained free of charge at http://www.ccdc.cam.ac.uk/conts/retrieving.html or from the Cambridge Crystallographic Data Center, 12, Union Road, Cambridge CB2 1EZ, UK. fax: (+44) 1223-336-033, email: deposit@ccdc.cam.ac.uk.

7. References

1. S. Chandrasekhar, P. Karri, *Tetrahedron Lett.* **2006**, *47*, 5763–5766. **DOI:**10.1016/j.tetlet.2006.06.006
2. T. Rosen, B. M. Trost, I. Fleming, C. H. Heathcock Eds., In comprehensive organic synthesis, Oxford: Peragmon 2, **1991**, 402–407.
3. G. P. Aguado, A. G. Monglioni, R. M. Ortuño, *Tetrahedron: Asymmetry* **2003**, *14*, 217–223. **DOI:**10.1016/S0957-4166(02)00749-8
4. (a) J. Plöchl, *Chem. Ber.* **1883**, *16*, 2815; **DOI:**10.1002/cber.188301602235 (b) J. Plöchl, *Chem. Ber.* **1884**, *17*, 1616. **DOI:**10.1002/cber.18840170215
5. F. Erlenmeyer, *Ann. Chem.* **1893**, 275.
6. G. Ozturk, S. Alp, S. Timur, *Dyes Pigm.* **2008**, *76*, 792–798. **DOI:**10.1016/j.dyepig.2007.02.005
7. K. M. Khan, U. R. Mughal, M. A. Lodhi, M. I. Choudhary, *Lett. Drug Des. Discovery*, **2008**, *5*, 52–56. **DOI:**10.2174/157018008783406624
8. K. M. Khan, U. R. Mughal, M. T. H. Khan, Zia-Ullah, S. Perveen, M. I. Choudhary, *Bioorg. Med. Chem.* **2006**, *14*, 6027–6033. **DOI:**10.1016/j.bmc.2006.05.014
9. M. A. Mesaik, S. Rahat, K. M. Khan, M. I. Choudhary, M. Shahnaz, Z. Ismaeil, Atta-ur-Rahman, A. Ahmad, Zia-Ullah, *Bioorg. Med. Chem.* **2004**, *12*, 2049–2057. **DOI:**10.1016/j.bmc.2004.02.034
10. S. İçli, A. O. Doroshenko, S. Alp, N. A. Abnamova, S. I. Egorova, A. S. Astley, *Spectrosc. Lett.* **1999**, *32*, 553–569. **DOI:**10.1080/00387019909350006

11. K. Ertekin, C. Karapire, S. Alp, B. Yenigül, S. Içli, *Dyes Pigm.* **2003**, *56*, 125–133. **DOI:**10.1016/S0143-7208(02)00125-0
12. Rigaku, CrysAlisPro Software System, Version 1.171.38.43. Rigaku Oxford Diffraction, **2015.**
13. G. M. Sheldrick, *Acta Crystallogr. Sect. A* **2015**, *71*, 3–8. **DOI:**10.1107/S2053273314026370
14. O. V. Dolomanov, L. J. Bourhis, R. J. Gildea, J. A. K. Howard, H. Puschmann, *J. Appl. Cryst.* **2009**, *42*, 339–341. **DOI:**10.1107/S0021889808042726
15. G. M. Sheldrick, *Acta Crystallogr. Sect. C* **2015**, *71*, 3–8. **DOI:**10.1107/S2053229614024218
16. K. K. Irikura, R. D. Johnson, III, R. N. Kacker, *J. Phys. Chem. A* **2005**, *109*, 8430–8437. **DOI:**10.1021/jp052793n
17. A. R. Katritzky, N. G. Akhmedov, A. Guven, J. Doskocz, R. G. Akhmedova, S. Majumder, C. D. Hall, *J. Mol. Struct.* **2006**, *787*, 131. **DOI:**10.1016/j.molstruc.2005.10.041
18. M. J. Frisch, G. W. Trucks, H. B. Schlegel, G. E. Scuseria, M. A. Robb, J. R. Cheeseman, G. Scalmani, V. Barone, B. Mennucci, G. A. Petersson, H. Nakatsuji, M. Caricato, X. Li, H. P. Hratchian, A. F. Izmaylov, J. Bloino, G. Zheng, J. L. Sonnenberg, M. Hada, M. Ehara, K. Toyota, R. Fukuda, J. Hasegawa, M. Ishida, T. Nakajima, Y. Honda, O. Kitao, H. Nakai, T. Vreven, J. A. Montgomery Jr., J. E. Peralta, F. Ogliaro, M. Bearpark, J. J. Heyd, E. Brothers, K. N. Kudin, V. N. Staroverov, T. Keith, R. Kobayashi, J. Normand, K. Raghavachari, A. Rendell, J. C. Burant, S. S. Iyengar, J. Tomasi, M. Cossi, N. Rega, J. M. Millam, M. Klene, J. E. Knox, J. B. Cross, V. Bakken, C. Adamo, J. Jaramillo, R. Gomperts, R. E. Stratmann, O. Yazyev, A. J. Austin, R. Cammi, C. Pomelli, J. W. Ochterski, R. L. Martin, K. Morokuma, V. G. Zakrzewski, G. A. Voth, P. Salvador, J. J. Dannenberg, S. Dapprich, A. D. Daniels, O. Farkas, J. B. Foresman, J. V. Ortiz, J. Cioslowski, D. J. Fox, Gaussian 09, Revision B.01, Gaussian, Inc., Wallingford CT, **2010**.
19. R. Dennington, T. Keith, J. Millam, GaussView, Version 5, Semichem Inc., Shawnee Mission, KS, **2009**.
20. Y. F. Sun, Y. P. Cui, *Acta Crystallogr. Sect. E* **2008**, *64*, o678. **DOI:**10.1107/S1600536808005746
21. A. M. Asiri, H. M. Faidallah, T. R. Sobahi, S. W. Ng, E. R. T. Tiekink, *Acta Crystallogr. Sect. E* **2012**, *68*, o1154. **DOI:**10.1107/S1600536812011579
22. M. Cygler, C. P. Huber, *Can. J. Chem*. **1986**, *64*, 2064–2067. **DOI:**10.1139/v86-341
23. R. Sevinçek, G. Öztürk, M. Aygün, S. Alp, O. Büyükgüngör, *J. Struct. Chem.* **2011**, *52*, 405–411. **DOI:**10.1134/S0022476611020247
24. N. Khelloul, K. Toubal, N. Benhalima, R. Rahmani, A. Chouaih, A. Djafri, F. Hamzaoui, *Acta Chim. Slov.* **2016**, *63,* 619-626. **DOI:**10.17344/acsi.2016.2362
25. R. Sevinçek, M. Aygün, S. Alp, C. Kazak, *J. Chem. Crystallogr.* **2011**, *41*, 1140–1144. **DOI:**10.1007/s10870-011-0059-x
26. S. Karmakar, A. N. Talukdar, *Indian J. Phys. A* **2004**, *78*, 923–925.
27. Y. F. Sun, X. L. Wang, J. K. Li, Z. B. Zheng, R. T. Wu, *Acta Crystallogr. Sect. E* **2007**, *63*, o4426. **DOI:**10.1107/S1600536807051458
28. M. Parveen, F. Ahmad, A. M. Malla, S. Azaz, M. R. Silva, P. S. P. Silva, *RSC Adv.* **2015**, *5*, 52330–52346.
29. R. Sevinçek, G. Öztürk, M. Aygün, M. Y. Ergün, S. Alp, O. Büyükgüngör, *Spectrosc. Lett.* **2009**, *42*, 1–6. **DOI:**10.1080/00387010802428708
30. K. N. Subbulakshmi, B. Narayana, H. S. Yathirajan, M. Akkurt, O. Çelik, C. C. Ersanlı, C. Glidewellg, *Acta Crystallogr. Sect. C* **2015**, *71*, 742–751. **DOI:**10.1107/S2053229615013637
31. A. M. Asiri, S. W. Ng, *Acta Crystallogr. Sect. E* **2009**, *65*, o1746. **DOI:**10.1107/S1600536809024593
32. V. G. Kasradze, E. V. Salimova, F. Z. Galin, O. S. Kukovinets, Z. A. Starikova, M. Yu. Antipin, *J. Struct. Chem.* **2010**, *51*, 599–602. **DOI:**10.1007/s10947-010-0089-9
33. J. Bernstein, R. E. Davis, L. Shimoni, N. L. Chang, *Angew. Chem. Int. Ed. Engl.* **1995**, *34*, 1555–1573. **DOI:**10.1002/anie.199515551
34. M. Govindarajan, S. Periandy, K. Carthigayen, *Spectrochim. Acta A* **2012**, *97*, 411–422. **DOI:**10.1016/j.saa.2012.06.028
35. E. Scrocco, J. Tomasi, *Adv. Quantum. Chem.* **1978**, *103*, 115–193. **DOI:**10.1016/S0065-3276(08)60236-1
36. İ. E. Kıbrız, Y. Sert, M. Sacmacı, E. Sahin, İ. Yıldırım, F. Ucun, *Spectrochim. Acta A* **2013**, *114*, 491–501. **DOI:**10.1016/j.saa.2013.05.022
37. R. M. Silverstein, G. C. Bassler, T. C. Morrill, Spectrometric identification of organic compounds, Fifth Ed., John Wiley and Sons Inc., Singapore, **1991**.
38. B. Kirste, *Chem. Sci. J.* **2016**, *7*, 127–131. **DOI:**10.4172/2150-3494.1000127

Povzetek

V okviru predstavljene raziskave smo s kondenzacijo *p-N,N*-dietilaminobenzaldehida z dvema derivatoma hipurne kisline sintetizirali dva oksazol-5-onska derivata, $C_{20}H_{20}N_2O_2$ (**1**) in $C_{21}H_{22}N_2O_2$ (**2**); oba smo v nadaljevanju študije tudi spektrokemijsko analizirali. Molekulski in kristalni strukturi smo določili z rentgensko difrakcijo monokristalov; izkazalo se je, da sta strukturi obeh kristalov stabilizirani s šibkimi intra- in intermolekularnimi interakcijami, kot tudi s C–O···π, C–H···π and π···π interakcijami. Računske študije smo izvedli z DFT metodo na nivoju B3LYP/6-311G(d,p). Izračunali smo vibracijske konstante in kemijske premike ter jih primerjali z eksperimentalnimi podatki. Simulirali smo tudi mejne molekulske orbitale in molekulske elektrostatske potencialne površine. Izračunani rezultati so pokazali, da se računsko optimizirani geometriji zelo dobro skladata z eksperimentalnima rezultatoma, dobljenima iz kristalne strukture. Namen je bil tudi ugotoviti učinek različnih reaktantov na kondenzacijo do oksazol-5-onov, na njihove značilne lastnosti in kristalne oblike končnih produktov.